Original Research Article

Study of the influence of the operational parameters on the photoelectro-Fenton performance of an industrial wastewater treatment prototype using Orange II as a model pollutant

Irma Robles [a], Francisco J. Rodríguez-Valadez [a], Eduardo Castaño [b], Luis A. Godínez [a, *]

[a] Center for Electrochemical Science and Technology (CIDETEQ), Pedro Escobedo, Querétaro 76703, Mexico
[b] Chemistry Department, Universidad Autónoma de Querétaro, Querétaro 23847, Mexico

ABSTRACT

A two-stage photoelectro-Fenton reactor was built and employed to test its ability to remove colour using Orange II as a model dye compound. A set of four critical operational variables was defined for the reactor under study. In order to quantify their significance on colour removal, a 2^4 experimental factorial design was used. From the resultant data, and from a variable interaction analysis, a model of the reactor's performance as well as a characteristic set of experimental conditions was obtained. From this information, a triple interaction among current density, resin concentration and pH was statistically significant. Hydraulic retention time was not important. The best treatment among those studied was obtained at pH 3, current density 23.9 mA cm^{-2}, and 3.7 g L^{-1} of resin concentration, with 96% decolorization. The best results with decolorization higher than 86% were obtained at acidic or slightly acidic pH, and higher levels of current density and resin concentration, or lower level of current density and resin concentration.

© 2016 Chinese Institute of Environmental Engineering, Taiwan. Production and hosting by Elsevier B.V. This is an open access article under the CC BY-NC-ND license (http://creativecommons.org/licenses/by-nc-nd/4.0/).

1. Introduction

Water availability for human consumption is rapidly becoming a major concern all around the world and therefore, there is an increasing need to develop wastewater treatment technologies capable of cleaning water and making it suitable for recycling. Among the most challenging water pollutants, organic dyes stand out due to their appearance and toxicity and therefore, fast and efficient contaminant oxidation processes are required. In this regard, the so-called Advanced Oxidation Processes (AOPs) constitute a good alternative for complicated aqueous effluents and several research groups around the world have been actively working and publishing on the subject [1–3]. AOPs are characterized by the generation and use of the hydroxyl radical species (HO•); a chemical that is capable of oxidizing a wide variety of organic pollutants at a fast rate [4–7].

There are many alternatives to generate the HO• radical species and one of the most popular ones is the use of the Fenton reagent.

This is an aqueous mixture of H_2O_2 and Fe^{2+} ions that, according to Eq. (1), is capable of producing the hydroxyl radical species,

$$Fe^{2+} + H_2O_2 \rightarrow Fe^{3+} + HO^• + OH^- \quad (1)$$
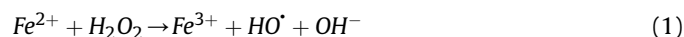
The process however, requires maintaining a relatively constant concentration of the components of the Fenton mixture, thus rendering the process unsuitable for most practical applications [8–10]. In order to overcome this problem, efforts have been devoted to design processes that avoid the need to feed the treating solution with expensive and difficult to handle H_2O_2 solutions, and to eliminate the need to separate and deal with the iron containing effluent once the polluted solution has been treated. Among these approaches, the electro-Fenton technology stands out as one of the most promising AOPs. In this process, while the H_2O_2 species is electrochemically generated by the $2e^-$ reduction of oxygen in solution as shown in Eq. (2),

$$O_2 + 2H^+ + 2e^- \rightarrow H_2O_2 \quad (2)$$

Iron ions are incorporated into the system by means of an iron loaded ion-exchange resin [11]. In order to increase the efficiency of the process, UV light can also be employed to promote the re-
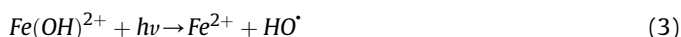
generation of ferrous ions by reduction of the ferric ionic species (Eq. (3)) produced by the Fenton mixture reaction (Eq. (1)) [8,9,11].

$$Fe(OH)^{2+} + h\nu \rightarrow Fe^{2+} + HO^{\bullet} \qquad (3)$$

Using these concepts, an industrial prototype with four identical photoelectro-Fenton reactors was constructed (Fig. 1a). Considering only one of these reactors (Fig. 1b), H_2O_2 is electrochemically produced in a first stage by reduction of dissolved oxygen as shown in Eq. (2). By switching a valve, a subsequent second stage takes place in which the H_2O_2 solution is passed through a UV radiated iron containing column to promote the generation of an oxidant dissolved species that is added to an Orange-II dye aqueous solution. The oxidation power of the aqueous solution prepared in the prototype was evaluated from the decrease of the spectroscopic absorbance signal of the dye in the aqueous mixture.

In order to optimize the prototype's performance, and since its operation involves the occurrence and coupling of electro-, photoelectro-chemical and chemical reactions that depend on the operating values of a set of key parameters, a study aimed to describe the relationship between these variables and the consequent optimal operation conditions of the prototype was carried out. For this purpose, an Orange II solution was used to model the prototype performance. The results of this study will not only define the operation of this reactor but also help understand the relative weight of the different parameters that control a typical photoelectro-Fenton process, thus allowing better judgement calls for the design and construction of AOP-based reactors.

2. Materials and methods

2.1. Chemicals

While Orange-II sodium salt (4-(2-Hydroxy-1-naphthylazo) benzene sulfonic acid sodium salt, $\geq$ 98%) was obtained from Fluka-Analytical with sodium- and ferrous-sulphate from J.T. Baker and used without further purification. Sulphuric acid (95% purity) on the other hand, was obtained from Karal, Industrial grade Oxygen gas was purchased from INFRA, carbon cloth was obtained from Electro-Chem Inc., and the iron loaded ion exchange resin (Purolite C-100) was obtained and prepared as previously reported [11]. All the solutions employed in this work were prepared using type I water (0.056 $\mu S\ cm^{-1}$), according to ASTM-D1193-99 [12].

2.2. Experimental procedures

Solutions for this study consisted on 10 L of 0.05 M Na_2SO_4 aqueous electrolyte (pH 7, I = 0.15) taken to pH 3 or 5 with H_2SO_4 as needed. Before introducing the solution in the reactor, oxygen saturation conditions were achieved by bubbling oxygen gas for 20 min.

As shown in Fig. 1b, a first stage of the process was used to circulate the electrolytic solution for 3.5 h trough the electrochemical reactor to promote the reduction of O_2 in a carbon cloth electrode (57 cm^2 perpendicular to flow direction) to achieve 30 ± 2 ppm concentration of H_2O_2 (Eq. (2)) [6]. By switching a valve, this solution is then pumped in a second stage (Fig. 1b) through a UV irradiated (mercury lamp, P = 75 mW cm^{-2}, λ = 365 nm, UVP Inc.) column filled with an iron-loaded-resin to generate the oxidant containing solution (Eqs. (1) and (3)). The oxidant containing electrolyte was then poured in an Orange-II dye containing solution, 50 mg L^{-1} in a 1:1 or 1:2 volume relationships and the absorbance of the resulting aqueous mixture (λ = 485 nm) was measured after 2.5 and 24 h to assess the oxidation power of electrolyte. Absorbance measurements were carried out using an Ocean Optics DT-mini-2 spectrophotometer (Boston, USA) at room temperature.

3. Results and discussion

3.1. Selection of the operational variables and their analysis window

The first step of this study consisted of identifying a set of operational variables capable of defining the performance of the photoelectro-Fenton reactor under study. These operational variables were chosen as pH, current density (mA cm^{-2}), hydraulic retention time (HRT, h) and the resin concentration (g L^{-1}), which works as a ferrous ion source for the Fenton reaction, and those variables were considered as the minimum set of quasi-independent variables from which all the other operational variables and the reactor's performance could be defined. In order to identify the working window of these operational variables however, a series of exploratory tests were carried out to define the ranges to be used in the design of experiments (DOE).

In this way, the energy required to promote hydrogen peroxide production from oxygen reduction (Eq. (2)) was the first and most straightforward variable to be considered. In order to assess the interfacial operating energy at the cathodic surface, Cyclic
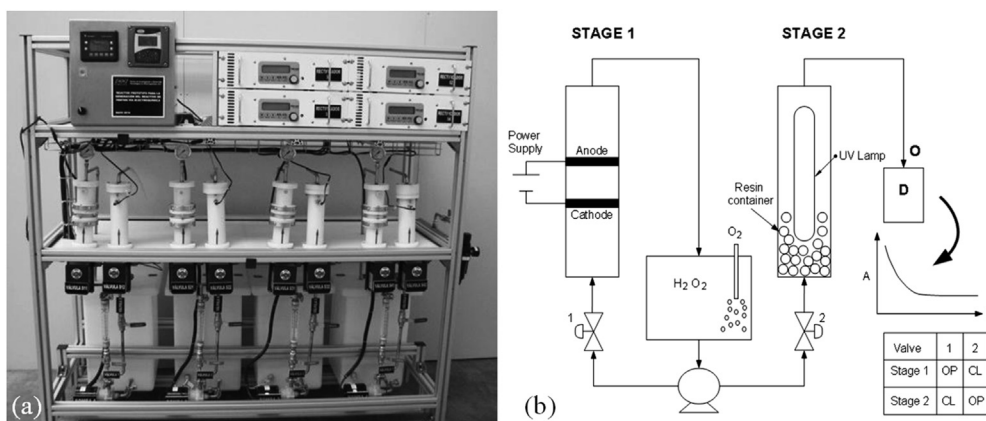

Fig. 1. (a) Industrial prototype for generation of the oxidant solution and (b) schematic description of the system along with the two stage operation process for the production of the oxidant rich aqueous solution.

Voltammetry (CV) experiments were carried out in the absence and in the presence of oxygen using the reactor chamber shown in Fig. 1. In these experiments, either O_2 or N_2 saturated solutions were studied using a couple of parallel-arranged carbon cloths functioning as working and counter electrodes, and a $Hg|Hg_2SO_4$ (Mercury|Mercurous Sulphate Electrode, MSE) as a reference electrode. As can be seen in Fig. 2a, comparison of the two resulting CV signals shows that oxygen reduces at about −1 V vs MSE.

For industrial electrochemical reactors, however, potential control is expensive and the current, closely related to the potential, is usually the parameter that is controlled. In this way, fixing the current establishes an interfacial potential at the cathode surface and therefore, experiments correlating different applied current values with stable cathodic potentials were performed. The tests carried out also reveal that the cathodic potential depends also on the solution HRT that circulates trough the reactor's chamber. As can be seen in Fig. 2b, the experimental surface that results from experiments considering not only current densities but different aqueous solution HRT as well shows that the region in which the potential is appropriate to selectively reduce O_2 to H_2O_2 (cathodic potential between −0.9 and −1.2 V) corresponds to current values in the 23.9–31.8 mA cm^{-2} range coupled to HRT between 9×10^{-3} and 4.5×10^{-3} h (red zone in the response surface of Fig. 2b).

To define the iron-loaded resin concentration [8] needed to effectively promote the generation of the oxidant species, decolorization tests of Orange-II (50 mg L^{-1}) using H_2O_2 (30 mg L^{-1}) solutions and varying amounts of the iron resin concentration (from 3.7 to 18.5 g L^{-1}) were carried out. From these experiments it was found that while 3.7 g L^{-1} of iron loaded resin concentration resulted in a 94% decolorization after 30 min; 7.4, 11.1 and 14.8 g L^{-1} resulted in 95, 75 and 30% decolorization values in the same experimental time, respectively. These results are consistent with literature reports that show that Fe ions in excess actually limit the decolorization efficiency of the process due to a cation oxidant scavenger effect [13,14]. Based on these experiments, the range for the resin concentration was chosen to be between 3.7 and 7.4 g L^{-1}.

pH on the other hand is a variable that is important to explore. It is well known that the electro-Fenton reaction works well under lightly acidic pH conditions (around 3) [8,9,15,16] not only because

of iron ion solubility but also because, as shown in Eq. (1), protons are required to produce H_2O_2 from oxygen reduction. Due to the practical nature of this work however, and considering the costs associated to acidification and subsequent neutralization of the effluent to be treated, a pH range from 3 to 7 was selected being aware that the reduction in acid/base costs at neutral pH values would necessarily result in a reduction on the production and efficiency of the oxidant species.

3.2. Experimental design

Therefore, the effects from pH, HRT (h), current density (mA cm^{-2}) and resin concentration (g L^{-1}) on colour removal were assessed using the completely randomized 2^4 factorial design shown in Table 1; two values that defined the experimental region (low and high levels, represented as (−) and (+), respectively) were selected for each one of the four operational variables identified, and a 2^4 factorial design, using four central points (denoted as (0) and defined as the middle value between the selected levels), was established. In this way, while the low and high levels for each one of the four variables were selected as 3 and 7 for pH, 4.5×10^{-3} and 9×10^{-3} h for HRT, 23.9 and 31.8 mA cm^{-2} for current density and 3.7 and 7.4 g L^{-1} for iron-loaded resin concentration, the four middle point values for each one of the four variables were the average between the high and low levels. To check for reproducibility, the 18 experiments resulting from this DOE (Table 1) were carried out twice and in order to avoid any tendency in the results related to an unwilling systematic error in the experimental order imposed by the experimentalist [15,17–23], the experiments were randomly performed.

The set of operational variables in any given experimental run of Table 1 results in a performance measure of the reactor that is directly related to the production of oxidant species, and assessed in terms of the colour decrease (% Y) of an Orange-II dye aqueous solution. As Eq. (4) shows, the response variable for the DOE is expressed in terms of the decolorization efficiency (Eq. (4)),

$$\%Y = \frac{A_0 - A_f}{A_0} \times 100 \qquad (4)$$
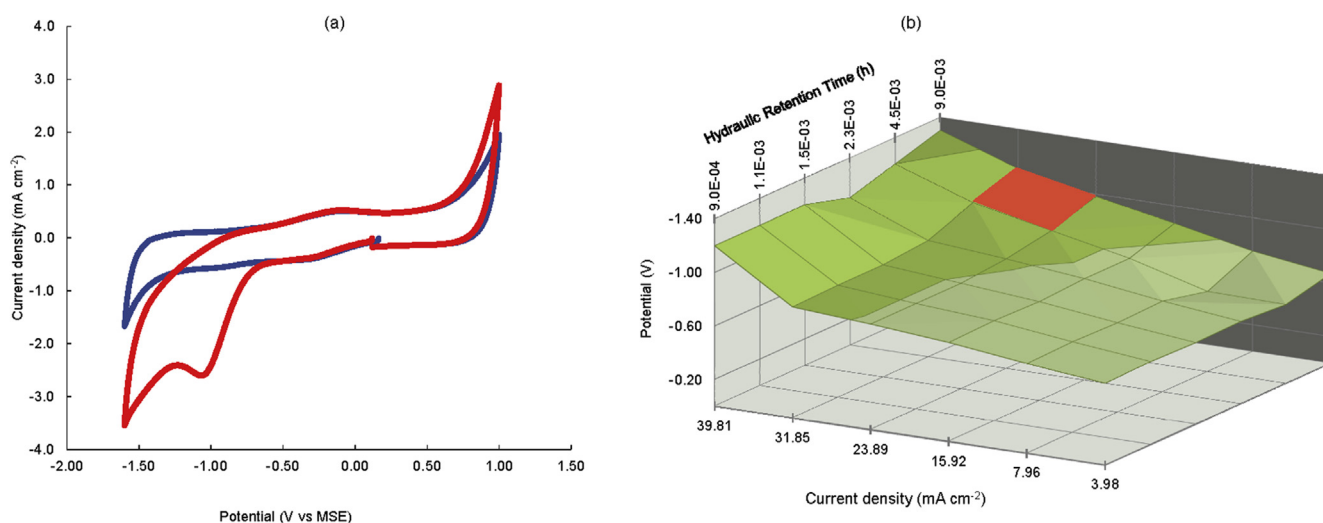
Fig. 2. (a) Cyclic Voltammetry of an aqueous solution contained in the electrochemical reactor shown in Fig. 1 in the absence (blue line) and in the presence (red line) of oxygen saturation conditions. Experiments carried out using carbon cloth, $Hg|Hg_2SO_4$ and Pt wire as work, reference and counter electrodes respectively. Scan rate 25 mV s^{-1}. (b) Potential-current-flow rate response surface in the presence of oxygen for the reactor shown in Fig. 1. The red square shows the region in which H_2O_2 generation through Eq. (1) is favoured.

Table 1
Experimental design used, all the experiments were randomized and carried out twice.

Run	pH	Hydraulic retention time ($\times 10^{-3}$ h)	Current density (mA cm^{-2})	Resin concentration (g L^{-1})
1	3	9	23.9	3.7
2	7	9	23.9	3.7
3	3	4.5	23.9	3.7
4	7	4.5	23.9	3.7
5	3	9	31.8	3.7
6	7	9	31.8	3.7
7	3	4.5	31.8	3.7
8	7	4.5	31.8	3.7
9	3	9	23.9	7.4
10	7	9	23.9	7.4
11	3	4.5	23.9	7.4
12	7	4.5	23.9	7.4
13	3	9	31.8	7.4
14	7	9	31.8	7.4
15	3	4.5	31.8	7.4
16	7	4.5	31.8	7.4
17 (0)	5	6	27.9	5.5
18 (0)	5	6	27.9	5.5

where A_0 and A_f, represent the absorbance of the original and the treated dye solution, respectively. Since the absorbance percentage decrease of the Orange-II species depends not only on the amount of oxidant generated in the reactor but also on the time in which the oxidant and the dye chemicals have reacted, measurements of (% Y) were made for each experimental run shown in Table 1 after 2.5 and 24 h. These reaction time values were selected from experiments in which it was observed that while at 2.5 h there were important colour differences between each run and absorbance was still changing, at 24 h the colour of the solutions was stable and therefore no further decolorization reactions were taking place after this time. It is also important to note that control experiments in which no current was applied to the reactor and therefore no oxidant species were generated in the reactor, showed that colour changes in the dye solution were, as expected, associated only to dilution effects.

3.3. Experimental data and performance analysis of the reactor under study

As described in the experimental design section, absorbance decrease data were collected using 1:1 and 1:2 (volume) electrolyte: dye solution. While both electrolyte:dye dilution ratios showed the expected proportional decolorization results, 1:1 dilution results showed higher deviation between replicates, and thus 1:2 volume ratio results were used for analysis.

In this way, Fig. 3 shows the decolorization efficiency results for the different sets of operational variables using the 1:2 electrolyte:dye dilution ratio at two different sampling times. Inspection of the resulting data shows that while at shorter reaction times (2.5 h $\times 10^{-3}$ h, Fig. 3a) there are smaller decolorization efficiencies and more variation of the results of the different sets of variables considered in the DOE, at longer times (24 $\times 10^{-3}$ h, Fig. 3b) most of the experimental treatments presented a decolorization higher than 75%, coupled with smaller variation of the results. Since the idea was to compare the different treatments for the reactor under study, it was considered that while the best treatments could be identified using the data that contained more information about the differences between the treatments shown in Table 1, i.e., at a shorter reaction time, 2.5 h (see Fig. 3a), the worst treatments could be identified under exhausted conditions in experiments carried out considering 24 h reaction times (see Fig. 3b).

Using this consideration, inspection of Fig. 3a reveals that the best treatments (best colour removal efficiencies (above 75%) at 2.5×10^{-3} h) correspond to runs 1, 13, 15, and 17, which are related to 96, 80, 94 and 86% decolorization efficiencies, respectively. In general terms, these high efficiencies are observed when pH values are slightly acidic (5 or 3).

The worst treatments on the other hand, were identified from the data in Fig. 3b in which decolorization efficiency below 75% could be observed for treatments 2 and 8 (60 and 53% decolorization efficiency, respectively). It is important to notice that these
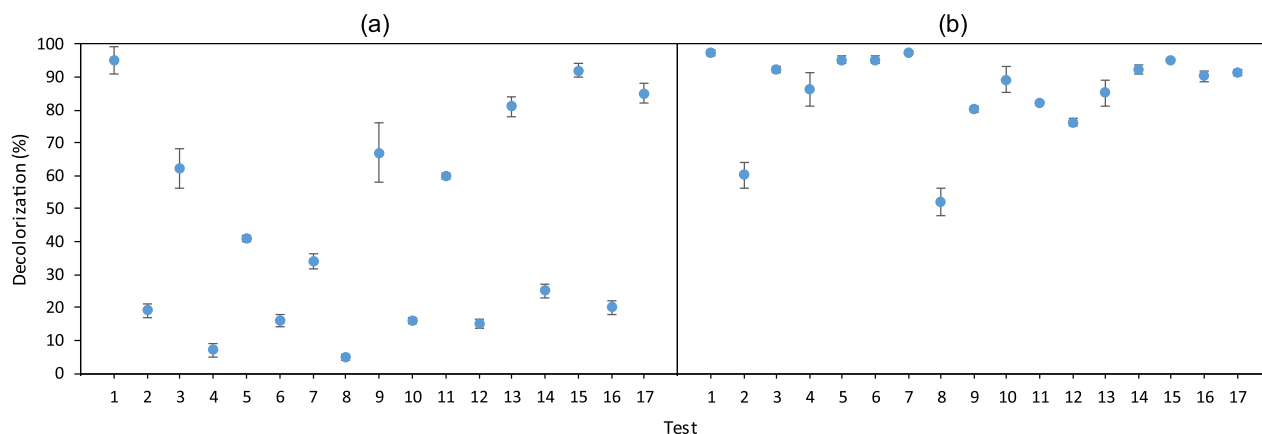
Fig. 3. Decolorization efficiency results for 1:2 electrolyte: dye ratio, after (a) 2.5 h, and (b) 24 h.

inefficient conditions are attained at high pH (neutral) values and low resin concentration levels.

From the data in Fig. 3, the response surface graphs shown in Fig. 4 were obtained. Fig. 4a and b shows the performance of the decolorization efficiency as a function of current and the amount of iron-loaded resin at the two different HRTs under acidic conditions, Fig. 4c and d shows the corresponding behaviour under neutral conditions. Inspection of Fig. 4a shows that when HRT is the highest $(9 \times 10^{-3}\,\text{h})$, the highest decolorization efficiency is obtained at low current density and resin concentration values. In a symmetrical way, Fig. 4b shows that when HRT is the lowest $(4.5 \times 10^{-3}\,\text{h})$, the decolorization efficiency is optimized when the current and the concentration of iron-loaded resin are high. In this way, at low current values, the best treatment is achieved when high HRTs are employed so that enough time is available for oxygen molecules to react at the electrode surface to achieve maximum H_2O_2 electrochemical synthesis. At lower HRT on the other hand, the electrochemical oxygen reduction reaction (Eq. (2)) is favoured when larger current values are applied.

For the amount of iron-loaded resin, the same tendency of that of current is observed. For instance, better decolorization performances of the reactor are observed when larger resin quantities are coupled with larger HRT or when lower amounts of resin are employed under lower HRT conditions.

The $HRT -$ current density-resin concentration relationships observed and described are consistent with a process in which the electrochemical reduction of oxygen to produce H_2O_2 is the efficiency-limiting factor. The fundamental role that plays the electrochemical oxygen reduction stage can also be inferred from comparison of the response surfaces of Fig. 5a and b, with those shown in Fig. 5c and d with the same conditions of HRT, resin concentration and current density under neutral pH conditions. This comparison clearly shows, not only poor decolorization performance of the reactor at high pH (always less than 30%) but also a low influence of the interaction between the resin concentration,
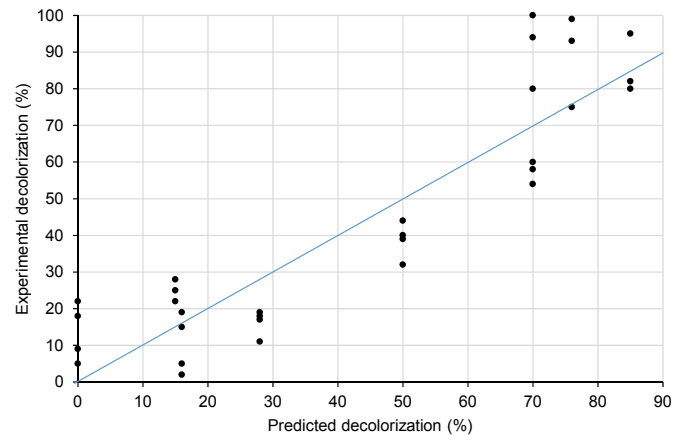

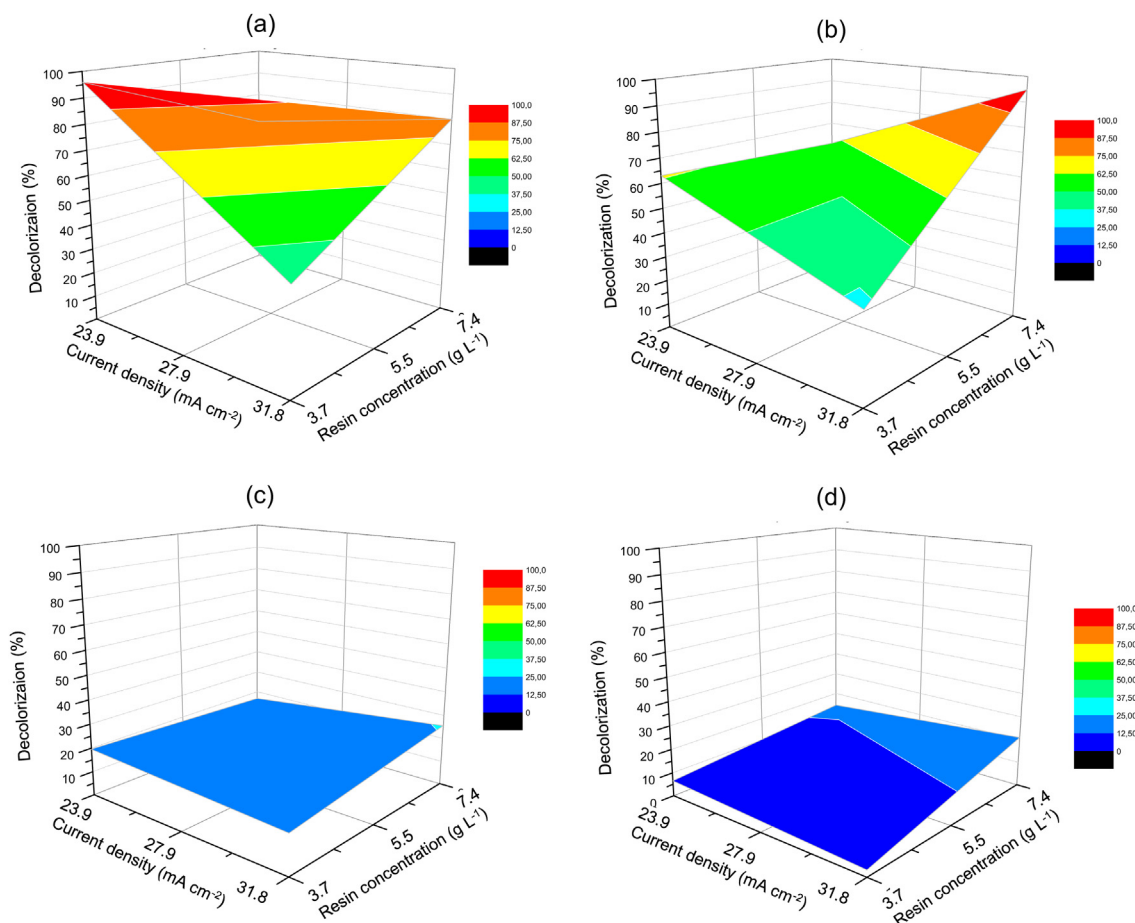**Fig. 5.** Experimental vs predicted results using Eq. (5).

Fig. 4. Experimental surface responses of decolorization as a function of current density and resin concentration at two pH and two HRT values. (a) pH = 3, HRT = 9×10^{-3} h, (b) pH = 3, HRT = 4.5×10^{-3} h, (c) pH = 7, HRT = 9×10^{-3} h, and (d) pH = 7, HRT = 4.5×10^{-3} h.

current density and HRT; a fact that is fully consistent with a pH dependent H_2O_2 generation step (Eq. (2)) that controls the overall performance of the reactor.

In order to get a better data interpretation, a second-order regression model was estimated using the statistical software JMP 7.0.2, SAS Institute [24]. The results of this analysis are shown in Table 2 and from the resultant data, an equation that models dye colour removal due to oxidant generation at the prototype could be obtained (Eq. (5)).

$$
\begin{aligned}
discoloration(\%) =\ & 140.18 - 13.12(pH) \\
& - 10.65(pH - 5)(pH - 5) \\
& - 28.01(12.56)(current\ density) \\
& + 12.85(0.27)(re\sin\ concentration) \\
& + 24.28((12.56)(current\ density) \\
& - 0.35)(pH - 5) - 139.46((12.56) \\
& \times (current\ density) - 0.35)(pH - 5)((0.27) \\
& \times (re\sin\ concentration) - 1.5)
\end{aligned}
$$

(5)

As can be seen in the predicted vs experimental data shown in Fig. 5 for all the experiments carried out, Eq. (5) is characterized by a relative low value of $R^2_{fit} = 0.81$ which renders the fitted relationship as a non-predictive semi-empirical correlation that can not be used to accurately predict the decolorization decrease for a given set of operational variables.

As can be seen in Fig. 5 however, the correlation is useful to roughly identify operational variable combinations that can be predicted to perform better than others and to assess to some extent the tendency of reactor performance if any given variable is changed within the window considered for this study. In fact and as can be seen in Fig. 5 and Table 3, the experimental and predicted data point out the same best and worst treatment combinations of

the performance of the reactor under study as those identified in the previous section.

The statistically significant effects in this model (Eq. (5)) are pH, resin concentration, the double interaction of resin concentration-current density and the triple interaction among pH, current density and resin concentration. The only effect to be interpreted is this triple interaction because pH, resin concentration and current density are their parenteral effects [23–29].

Variable interaction analysis makes possible to show synergies or antagonisms among variables. As can be seen from the data presented in Table 2, the interactions for which the Prob > ltl being 0.05 or less, are those corresponding to pH, resin concentration and the pH-current density-resin concentration interaction parameters.

It is interesting to note that the HRT does not seem to play a crucial role in the interactions directly related to the decolorization efficiency measured in the experiments shown in Table 1. Consistent with the data analysis presented in the previous section, the HRT does not appear in the interaction results of Table 2 since its influence is eliminated with the combination of pH, current density and resin concentration that maximizes the electrochemical-chemical generation of the oxidant species under acidic conditions when either low HRT, low current density or low resin concentration is used or when high HRTs are associated with high values of current density and resin concentration.

When HRT is eliminated from the description of the reactor's behaviour either by the analysis of the experimental data or by inspection of the variable interaction analysis results of Table 2, it is possible to use Eq. (5) to generate the surface response curves presented in Fig. 6. Although these curves cannot reflect the precise reactor performance under any given set of operational variable conditions, they can give a good idea of the tendency and influence of the working variables. In this way, and consistent with the experimental results previously discussed, inspection of Fig. 6 reveals that at low pH values (Fig. 6a), the decolorization efficiency is high at low applied currents and independent on the resin concentration employed. At high values of applied current on the other

Table 2
Estimated parameters of the regression model.

Term	Estimated	Standard error	T ratio	Prob > |t|
Intercept	114.06	27.28	4.18	0.0005
pH	−13.12	1.58	−8.28	<0.0001*
HRT (Hydraulic Retention Time)	−16.95	12.67	−1.34	0.20
(pH-5)*(HRT-0.75)	0.15	6.34	0.02	0.98
Current Density	−28.01	63.36	−0.44	0.66
(pH-5)*(Current Density-0.35)	24.28	31.68	0.77	0.45
(HRT-0.75)*(Current Density −0.35)	208.13	253.45	0.82	0.42
(pH-5)*(HRT-0.75)*(Current Density −0.35)	−113.44	126.72	−0.90	0.39
Resin Concentration	12.85	6.34	2.03	0.06*
(pH-5)*(Resin Concentration −1.5)	−2.40	3.17	−0.76	0.46
(HRT-0.75)*(Resin Concentration −1.5)	31.02	25.35	1.22	0.24
(pH-5)*(HRT-0.75)*(Resin Concentration −1.5)	−6.07	12.67	−0.48	0.64
(Current Density −0.35)*(Resin Concentration −1.5)	396.94	126.73	3.13	0.01*
(pH-5)*(Current Density −0.35)*(Resin Concentration −1.5)	−139.46	63.36	−2.20	0.04*
(HRT-0.75)*(Current Density −0.35)*(Resin Concentration −1.5)	−119.95	506.90	−0.24	0.82
(pH-5)*(HRT-0.75)*(Current Density −0.35)*(Resin Concentration −1.5)	42.43	253.45	0.17	0.87

Table 3
Comparison of obtained and calculated efficiency (Y), for the most and least efficient tests 1, 13, 15, 17, 2 and 8.

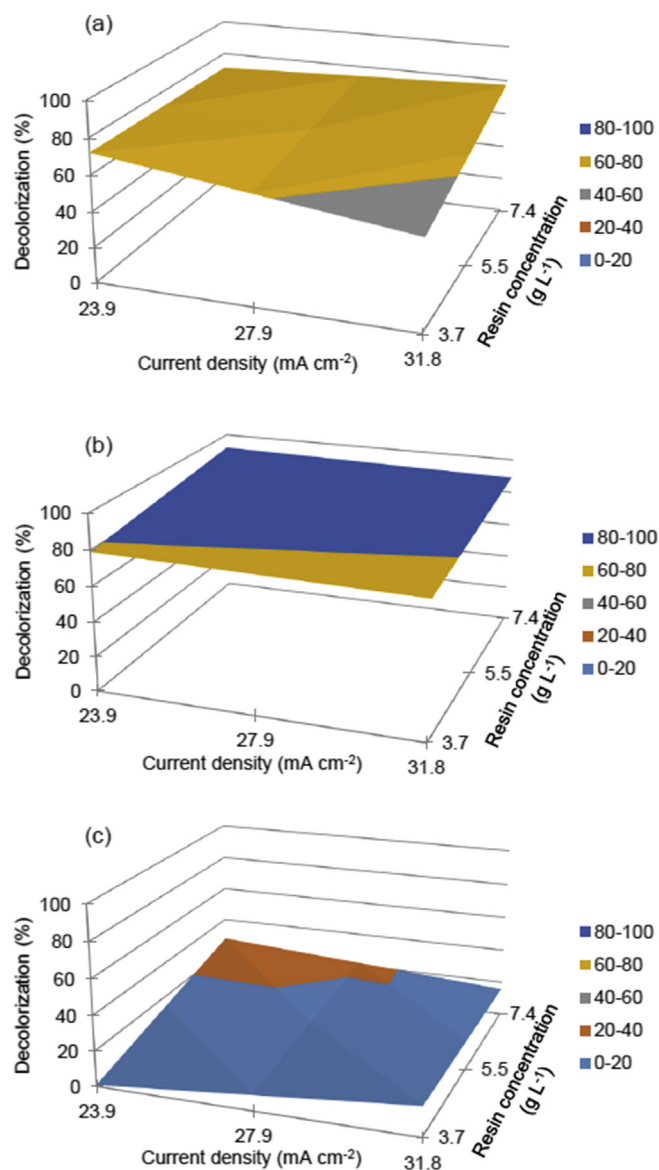| Test	pH	Hydraulic retention time ($\times 10^{-3}$ h)	Current density (mA cm^{-2})	Resin concentration (g L^{-1})	$Y_{experimental}$ (%)	$Y_{calculated}$ (%)
1	3	9	23.9	3.7	96	72
13	3	9	31.8	7.4	84	77
15	3	4.5	31.8	7.4	94	77
17	5	6	27.9	5.5	86	84
2	7	9	23.9	3.7	20	1
8	7	4.5	31.8	3.7	3	17

Fig. 6. Surface response curves predicted with Eq. (5), at different pH conditions, (a) pH = 3, (b) pH = 5, (c) pH = 7.

concentration is employed, it can also be seen that better results are expected at low applied current values.

4. Conclusions

A two-stage photoelectro-Fenton Prototype for industrial wastewater treatment was constructed and a critical set of operation variables was identified in order to define the working window for each variable. Using a DOE approach, it was possible to obtain a modelling equation for the oxidant production process and to obtain experimental and predicted surface response curves that describe the reactor's performance. Analysis of this information reveals that as expected, the electrochemical production of H_2O_2 and OH radicals in the electrochemical-chemical processes controls the oxidation power of the resulting solution. The studies also reveal that while the pH-current-resin interaction shows high influence in the response variable, the HRT does not have a substantial influence in decolorization efficiency. The consistency for electrochemical production of hydrogen peroxide using all high or all low values of current density, resin concentration and HRT seems to eliminate the in influence of the altering variable in the variable interaction analysis. Consistent with literature reports, pH 3 condition is more favourable for the processes than neutral conditions. In this regard, our experimental and predicted data reveal that under certain conditions pH 5 also constitutes a fairly good acidity level that reduces the cost of acidification/neutralization of the processes. For complex photoelectro-Fenton systems for industrial wastewater treatment, operational variable optimization is a challenge that can be approximated using the experimental design approach. Although its results are not predictive, the analysis can provide valuable criteria for the optimization of the working conditions of the reactor's operational variables.

hand, decolorization efficiencies are more sensitive to the amount of resin concentration employed and in fact the amount of resin is proportional to the decolorization efficiency. These tendencies are consistent with processes in which at low pH, H_2O_2 production is optimized at low current density (no influence of resin concentration) and at high current density the amount of H_2O_2 is smaller and the resin controls the amount of oxidant generated. As can be seen in Fig. 6b decolorization efficiencies are substantially lower than those observed at pH 7, using any combination of variables. In this case, the scarcity of protons to electrochemically produce H_2O_2 (see Eq. (2)), coupled to the formation of hydrated hydroxide species of iron in the resin chamber, prevents the formation the oxidant species responsible for the decolorization of the dye solution. Fig. 6c, on the other hand, shows the predicted behaviour of the performance of the electrochemical reactor at pH 5. It is interesting to note from comparison with Fig. 6a and b that as expected, the behaviour suggests an intermediate performance between that observed under acidic and neutral conditions. In this case, while the best performance is observed when larger resin

References

[1] Brillas E. A review on the degradation of organic pollutants in waters by UV photoelectro-Fenton and solar photoelectro-Fenton. J Braz Chem Soc 2014;25: 393–417.

[2] Sirés I, Brillas E, Oturan MA, Rodrigo MA, Panizza M. Electrochemical advanced oxidation processes: today and tomorrow. A review. Environ Sci Pollut Res 2014;21:8336–67.

[3] Brillas E, Martinez-Huitle CA. Decontamination of wastewaters containing synthetic organic dyes by electrochemical methods. An updated review. Appl Catal B Environ 2015;166–167:603–43.

[4] Ray MB, Chen JP, Wang LK, Pehkonen SO. Advanced oxidation processes. In: Wang LK, Hung YT, Shammas NK, editors. Advanced physicochemical treatment processes. Totowa, NJ: Humana Press; 2007. p. 463–81.

[5] Peralta-Hernández JM, Mejía S, Godínez LA, Meas-Vong Y. Fenton and electrochemical approaches for water purification technologies. In: Palomar M, Pandalai SG, editors. Applications of analytical chemistry in environmental research. Trivandrum, India: research Signpost; 2005. p. 101–30.

[6] Andreozzi R, Caprio V, Insola A, Marotta R. Advanced oxidation processes (AOP) for water purification and recovery. Catal Today 1999;53:51–9.

[7] Pera-Titus M, García-Molina V, Baños MA, Giménez J, Esplugas S. Degradation of chlorophenols by means of advanced oxidation processes: a general review. Appl Catal B Environ 2004;47:219–56.

[8] Neyens E, Baeyens J. A review of classic Fenton's peroxidation as an advanced oxidation technique. J Hazard Mater 2003;98:33–50.

[9] Peralta-Hernández JM, Meas-Vong Y, Rodriguez FJ, Chapman TW, Maldonado MI, Godínez LA. In situ electrochemical and photo-electrochemical generation of the fenton reagent: a potentially important new water treatment technology. Water Res 2006;40:1754–62.

[10] Bañuelos JA, Rodríguez FJ, Rocha JM, Bustos E, Rodríguez A, Cruz JC, et al. Novel electro-Fenton approach for regeneration of activated carbon. Environ Sci Technol 2013;47:7927–33.

[11] Ramírez J, Godínez LA, Méndez M, Meas Y, Rodríguez FJ. Heterogeneous photo-electro-Fenton process using different iron supporting materials. J Appl Electrochem 2010;40:1729—36.

[12] ASTM. Standard specification for reagent water. West Conshohocken, PA: American Society for Testing and Materials; 2011.

[13] Ruiz EJ, Hernández-Ramírez A, Peralta-Hernández JM, Arias C, Brillas E. Application of solar photoelectro-Fenton technology to azo dyes mineralization: effect of current density, Fe^{2+} and dye concentrations. Chem Eng J 2011;171:385—92.

[14] Panizza M, Oturan MA. Degradation of Alizarin Red by electro-Fenton process using a graphite-felt cathode. Electrochim Acta 2011;56:7084—7.

[15] Almeida LC, Garcia-Segura S, Bocchi N, Brillas E. Solar photoelectro-Fenton degradation of paracetamol using a flow plant with a Pt/air-diffusion cell coupled with a compound parabolic collector: process optimization by response surface methodology. Appl Catal B Environ 2011;103:21—30.

[16] Feng JY, Hu XJ, Yue PL. Effect of initial solution pH on the degradation of Orange II using clay-based Fe nanocomposites as heterogeneous photo-Fenton catalyst. Water Res 2006;40:641—6.

[17] Grčić I, Vujević D, Koprivanac N. The use of D-optimal design to model the effects of process parameters on mineralization and discoloration kinetics of Fenton-type oxidation. Chem Eng J 2010;157:408—19.

[18] Grujicic M, Zhao CL, Roy WN. A statistical analysis of the mechanical and electronic-transport properties of stochastic porous fibrous materials. J Mater Sci 2005;40:5181—90.

[19] Prasad RK. Degradation of biopolymeric pigments in distillery spentwash by electrocoagulation using copper anodes: statistical and canonical analysis. Environ Chem Lett 2010;8:149—55.

[20] Rodríguez M, Malato S, Pulgarin C, Contreras S, Curcó D, Giménez J, et al. Optimizing the solar photo-Fenton process in the treatment of contaminated water. Determination of intrinsic kinetic constants for scale-up. Sol Energy 2005;79:360—8.

[21] Merabet S, Robert D, Weber JV, Bouhelassa M, Benkhanouche S. Photocatalytic degradation of indole in UV/TiO_2: optimization and modelling using the response surface methodology (RSM). Environ Chem Lett 2009;7:45—9.

[22] Song Y, Kim D, Park Y. Statistical optimization of Rhodamine B removal by factorial design using reaction rate constant in electrochemical reaction. Korean J Chem Eng 2011;28:156—63.

[23] Cristóvão RO, Amaral PFF, Tavares APM, Coelho MAZ, Cammarota MC, Loureiro JM, et al. Optimization of laccase catalyzed degradation of reactive textile dyes in supercritical carbon dioxide medium by response surface methodology. React Kinet Mech Catal 2010;99:311—23.

[24] SAS-Incorporated. JMP 7.0.2. Cary, NC; 1998.

[25] Henquín ER, Bisang JM. Simplified model to predict the effect of the leakage current on primary and secondary current distributions in electrochemical reactors with a bipolar electrode. J Appl Electrochem 2005;35:1183—90.

[26] Salazar R, Garcia-Segura S, Ureta-Zañartu MS, Brillas E. Degradation of disperse azo dyes from waters by solar photoelectro-Fenton. Electrochim Acta 2011;56:6371—9.

[27] Burbano AA, Dionysiou DD, Suidan MT, Richardson TL. Oxidation kinetics and effect of pH on the degradation of MTBE with Fenton reagent. Water Res 2005;39:107—18.

[28] Spuhler D, Rengifo-Herrera JA, Pulgarin C. The effect of Fe^{2+}, Fe^{3+}, H_2O_2 and the photo-Fenton reagent at near neutral pH on the solar disinfection (SODIS) at low temperatures of water containing Escherichia coli K12. Appl Catal B Environ 2010;96:126—41.

[29] Nogueira RFP, Silva MRA, Trovó AG. Influence of the iron source on the solar photo-Fenton degradation of different classes of organic compounds. Sol Energy 2005;79:384—92.